



# Imbalanced testicular metabolism induced by thyroid disorders: New evidences from quantitative proteome

Samantha Nascimento Gomes<sup>1</sup> · Deborah Elzita do Carmo Corrêa<sup>1</sup> · Isabela Medeiros de Oliveira<sup>1</sup> · Paula Bargi-Souza<sup>2</sup> · Monica Degraf Cavallin<sup>1</sup> · Danielle Dobner Mariano<sup>1</sup> · Najeh Maissar Khalil<sup>3</sup> · David Livingstone Alves Figueiredo<sup>1</sup> · Marco Aurelio Romano<sup>1</sup> · Claudio Alvarenga de Oliveira<sup>4</sup> · Renata Marino Romano<sup>1</sup>

Received: 9 April 2019 / Accepted: 21 June 2019 / Published online: 29 June 2019  
© Springer Science+Business Media, LLC, part of Springer Nature 2019

## Abstract

Thyroid dysfunctions, such as hypothyroidism and hyperthyroidism, are the second most prevalent endocrinopathies and are associated to reproductive disorders in men. Several genes are differentially modulated by thyroid hormones in testes and imbalances in thyroid hormone levels are also associated to alterations on sperm functionality. Imbalances on antioxidant defense mechanism and stress oxidative have been pointed out as the main factors for the impairments on male reproductive function. To clarify this issue, we investigated the expression and activity of antioxidant enzymes in testis, followed by their proteomic profile in attempt to characterize the mechanisms involved in the alterations induced by hypo- or hyperthyroidism in adult male rats. Hypothyroidism reduced the *Gsr* transcript expression and the activity of CAT and GSR enzymes, while the hyperthyroidism reduced the *Gpx4 var2* transcript expression. Among 1082 identified proteins, 123 and 37 proteins were downregulated by hypothyroidism compared to euthyroid and hyperthyroid condition, respectively, being 36 proteins commonly reduced in both comparisons and one exclusively in hypo-hyperthyroidism comparison. A network containing 29 nodes and 68 edges was obtained in protein–protein interaction analysis and the functional enrichment analysis of differentially expressed proteins revealed significant alterations for several functions in hypo-euthyroid and hypo-hyperthyroid comparisons, such as ATP metabolic process, coenzyme binding, sperm part, peroxiredoxin activity, mitochondrial protein complex, intramolecular oxidoreductase activity, binding of sperm to zona pellucida, glutathione transferase activity, response to testosterone. Thus, there is a correlation between thyroid disorders and impaired antioxidant defense mechanism, resulting in reproductive dysfunctions, as infertility, mainly observed in hypothyroidism.

**Keywords** Male infertility · Sperm abnormalities · Antioxidant enzymes · Spermatogenesis · Hypothyroidism · Hyperthyroidism

**Supplementary information** The online version of this article (<https://doi.org/10.1007/s12020-019-01989-8>) contains supplementary material, which is available to authorized users.

✉ Renata Marino Romano  
romano@unicentro.br

<sup>1</sup> Grupo de Estudo e Pesquisa em Tireoide (GEPET), Department of Medicine, State University of Centro-Oeste (UNICENTRO), Rua Simeão Camargo Varela de Sa, 03, 85040-080 Parana, Brazil

<sup>2</sup> Department of Physiology and Biophysics, Institute of Biological Sciences, Federal University of Minas Gerais, Avenida Presidente Antônio Carlos, 6627, 31270-901 Minas Gerais, Brazil

## Introduction

Infertility is characterized by the failure to establish pregnancy after 12 months of regular and unprotected sexual intercourse and affects about 8 and 12% of couples in reproductive age worldwide, with men accounting for 50%

<sup>3</sup> Pharmaceutical Nanotechnology Laboratory, Department of Pharmacy, State University of Centro-Oeste (UNICENTRO), Rua Simeão Camargo Varela de Sa, 03, 85040-080 Parana, Brazil

<sup>4</sup> Laboratory of Hormonal Dosages, Department of Animal Reproduction, Faculty of Veterinary Medicine, University of Sao Paulo (USP), Av. Prof. Dr. Orlando Marques de Paiva, 87, 05508-270 Sao Paulo, Brazil

of these cases [1]. Although many conditions are related to the cause of men infertility, about 60% of the cases are still classified as idiopathic [2].

Thyroid hormones (TH) actions on testicles of adults has been a controversial issue discussed in the last decades, even though it is recognized that thyroid dysfunctions, such as hypothyroidism and hyperthyroidism, have negative impact on men fertility (recently reviewed by La Vignera, Vita [3]). Recently, the number of evidence of TH modulation of the hypothalamic-pituitary-testicular axis is increasing [4]. The global prevalence of thyroid dysfunction ranges 1–2% for hypothyroidism and 0.2–1.3% for hyperthyroidism in iodine-sufficient countries [5]. In a cross-sectional analysis of men seeking medical care for couple infertility, 3.7% and 7.4% presented subclinical hyperthyroidism and hypothyroidism, respectively [6], reinforcing the need to investigate and understand the TH action on adult testes.

The expression of thyroid related genes was previously assessed in adult hypo- or hyperthyroid rats by our group [7]. Hypothyroidism upregulates the transcript expression of Thyroid hormone receptor alpha 1 (*Thra1*), a critical mediator of TH transcriptional actions in testes [8]. On the contrary, the expression of deiodinase type III (*Dio3*), enzyme that converts thyroxine (T4) and triiodothyronine (T3) to reverse triiodothyronine (rT3) and diiodothyronine (T2), respectively, is downregulated in hypothyroidism [7]. Thus, molecular adjustments are triggered in testes increasing the intracellular response to TH and reducing the TH degradation, possibly in attempt to compensate the lower TH levels in hypothyroid condition [7]. In hyperthyroidism, the expression of thyroid hormone transporter, known as monocarboxylate transporter 8 (*Slc16a2*), is upregulated, possibly decreasing the intracellular excess of thyroid hormones in the testis [7].

Regarding the sperm functionality, both hypothyroidism and hyperthyroidism reduced the mitochondrial activity, while the acrosome integrity was reduced only in hypothyroid animals [7]. Together, these sperm alterations point out an imbalance between ROS generation and removal systems to avoid the oxidative stress which impair the fertilization process [9]. Indeed, previous studies using different experimental models or even in hypo- or hyperthyroid men showed that the imbalanced antioxidant defense mechanism in the testis is the major responsible for impairments on sperm functionality and quality [10–14]. Moreover, high content of polyunsaturated fatty acids (PUFA) in the plasma membrane makes the spermatozoa highly susceptible to oxidative damage [15] and the male infertility is associated with oxidative stress in the seminal plasma [16]. Besides that, it is known that the TH regulates the metabolism of several

tissues [17]. Thus, alterations in the testicles metabolism due to thyroid dysfunctions could also affect the spermatogenesis and sperm functionality.

In this sense, we first investigate the possible unbalances in the antioxidant defense mechanism through the evaluation of catalase (CAT), glutathione peroxidase (GPX), glutathione reductase (GPR) and superoxide dismutase (SOD) expression and enzymatic activity, followed by a proteomic profile of testis of rats in attempt to characterize the mechanisms involved in the alterations induced by hypo- or hyperthyroidism developed in the adulthood.

## Material and methods

### Experimental design

In total 36 90-day-old male Wistar rats (*Rattus norvegicus*) were randomly split into three groups and subjected to the following treatments: (a) euthyroid [control animals treated with saline, intraperitoneally (ip), and drinking water *ad libitum*]; (b) hypothyroid [surgical thyroidectomy followed by 0.03% methimazole (Sigma-Aldrich, USA) and 0.05% calcium chloride (CaCl<sub>2</sub>) in drinking water during 21 days]; or (c) hyperthyroid [1,5 µg T3/100 g of body weight (BW), twice a day, ip, from 105 to 109-day old; T3: 3,3',5-Triiodo-L-thyronine, T2877, Sigma-Aldrich, USA, drinking water *ad libitum*]. All rats were euthanized at 110-days-old and the tissues were collected. Surgeries and euthanasia were performed under deep anesthesia with 100 mg of ketamine plus 20 mg of xylazine per kg/BW, ip in bolus. The induction of hypothyroidism and hyperthyroidism was in accordance with thyroid experimental guidelines [18] and our previous study [7]. Animals were maintained into subgroups of four in polypropylene cages (43 × 43 × 20 cm) with a 5 cm layer of wood shavings, with rat chow (Nuvilab CR-1, Quimtia, PR, Brazil) under a 12:12 h dark/light cycle in a temperature-controlled room (22 ± 2 °C). All procedures were performed in accordance with the National Guidelines for Animal Experimentation and were approved by the Universidade Estadual do Centro-Oeste, Ethical Committee for Animal Research (protocol # CEUA 010/2014).

### Tissue collection

Blood was collected via cardiac puncture and centrifuged at 2191 × g (Excelsa II 206 BL, Sao Paulo, SP, Brazil) for 15 min. The serum was separated, frozen and stored at –70 °C for subsequent hormone evaluation. The hearts were excised, dehydrated for 24 h at 37 °C and weighed. Testes were quickly removed, pulverized in liquid nitrogen and maintained in ultrafreezer at –70 °C until use.

## Evaluation of thyroid status

The thyroid status of animals was assessed by the measurement of TSH and T3 serum concentrations and by the dehydrated heart weight compared to euthyroid animals, as previously described [19].

## Hormone measurements

The TSH and T3 serum concentrations were determined by a chemiluminescent immunoassay using Luminex xMAP technology (Milliplex MAP rat thyroid panel, Billerica, MA, USA), according to the manufacturer instructions by the Laboratório Especializado em Análises Científicas Ltda. (LEAC, Sao Paulo, SP).

## Reverse transcriptase followed by real-time quantitative PCR (RT-qPCR)

The mRNA expression of catalase (*Cat*), superoxide dismutase 1 (*Sod1*), glutathione-disulfide reductase (*Gsr*), glutathione peroxidase 4 transcripts variants 1 (*Gpx4var1*) and 2 (*Gpx4var2*) relative to ribosomal protein L19 (*Rpl19*) was evaluated in testis. For this, total RNA was extracted with TRIzol® Reagent (Life Technologies, Carlsbad, CA, USA) according to the manufacturer's instructions and its concentration was measured with a Kasvi nanospectrophotometer (Kasvi, Brazil). Total RNA (2.5 µg) was reverse transcribed for 60 min at 42 °C using oligo (dT) primer and GoScript Reverse Transcription System (Promega, Madison, USA), according to the manufacturer's instructions. Real-time PCR was carried out in 10 µL reaction volume with 10 ng of cDNA and a mix containing 2 µM of primers, 0.5 µM of ROX dye and 5 µL of Platinum® SYBR® Green qPCR SuperMix-UDG (Life Technologies, Carlsbad, USA). The amplification was performed using Applied Biosystems StepOnePlus™ Real-Time PCR System (Applied Biosystems, Singapore) following the cycle conditions: 50 °C (2 min), 95 °C (2 min), and 40 cycles of 95 °C (15 s) and 60 °C (30 s). At the end of the cycles, a melting curve was generated and analyzed to confirm the specificity of the amplification. The average cycle threshold (Ct) was automatically determined using StepOne™ Software v2.3 (Applied Biosystems) and quantification was performed by the  $2^{-\Delta\Delta C_t}$  method, as previously described [20]. The primer sequences are shown in Supplementary Table 1.

## Antioxidant enzyme activity in the testis

Twenty-five milligrams of pulverized testis was homogenized in a 250 µL of 0.5 mM Tris–HCl pH 7.4 and centrifuged at  $590 \times g$  during 10 min at 4 °C. The supernatant

was collected and the total protein content was estimated by Bradford method [21]. The supernatant was used in the enzymatic assays to determine the activities of superoxide dismutase, glutathione peroxidase, glutathione reductase and catalase. The superoxide dismutase activity was evaluated according to the manufacturer instructions of the RANSOD kit (Randox Laboratories Limited, Cruclin, Northern Ireland) and previously described [22]. The results were expressed as unit of SOD per microgram of protein (U of SOD  $\times \mu\text{g}$  of Ptn<sup>-1</sup>). The glutathione peroxidase activity was measured with the RANSEL kit (Randox Laboratories Limited, Cruclin, Northern Ireland) as previously published [23] and the results were expressed as unit of GPX per liter per microgram of protein (U of GPX  $\times \text{L}^{-1} \times \mu\text{g}$  of Ptn<sup>-1</sup>). The glutathione reductase activity was evaluated following the manufacturer instructions for the GLUT RED kit (Randox Laboratories Limited, Cruclin, Northern Ireland) as previously described [24, 25]. The results were expressed as unit of GSR per liter per microgram of protein (U of GSR  $\times \text{L}^{-1} \times \mu\text{g}$  of Ptn<sup>-1</sup>). The catalase activity was assessed by the hydrogen peroxide decay at 30 °C by spectrophotometry at 240 nm, according to previous studies [26]. The results were expressed as delta of absorbances (initial minus final) per second per µg of protein ( $\Delta \text{Abs} \times \text{Sec}^{-1} \times \mu\text{g}$  of Ptn<sup>-1</sup>).

## Statistical analysis

The variables were submitted to Kolmogorov–Smirnov tests for normality and the Bartlett test for homoscedasticity. The TSH serum concentration results were compared between the groups using Kruskal–Wallis nonparametric analysis followed by the post hoc Dunn test. All other parameters were analyzed by ANOVA test followed by the post hoc of Tukey. The analysis were performed with Statistica 7.0 (Statsoft Inc, Tulsa, OK, USA). Statistical differences were considered significant when *P* value was lower than 0.05. The values were expressed as means and the standard error of the mean ( $\pm \text{SEM}$ ) for parametric and median and interquartile ranges for nonparametric analysis.

## Quantitative proteomic profile of testis by nanoLC-Orbitrap mass spectrometry analysis

### Protein extraction

Hundred milligrams of pulverized testis were homogenized in 300 µL of RIPA buffer containing 50 mM Tris–HCl pH 8.0, 150 mM sodium chloride, 1.0% Igepal CA-630 (NP-40), 0.5% sodium deoxycholate, and 0.1% sodium dodecyl sulfate, with protease inhibitor cocktail (P8340, Sigma-Aldrich), incubated at 4 °C for 30 min and the samples were centrifuged at  $10,000 \times g$  during 10 min at 4 °C. Afterwards,

the supernatant was removed and the total protein content was determined [21].

### Trypsin digestion

Fifty micrograms of supernatant were digested with trypsin (in-solution). Briefly, the protein was dissolved in urea and the pH was adjusted to 8.0–9.0 with  $\text{NH}_4\text{HCO}_3$ . The samples were reduced with 10 mM dithiothreitol (DTT) for 30 min at 37 °C in the thermomixer at 100 rpm. The samples were alkylated for 30 min in the dark at room temperature in the presence of 50 mM iodoacetamide, followed by a digestion for 16 h at 37 °C with trypsin (1:50) (Trypsin Gold, Mass spectrometry grade, Promega, WI, USA) in digestion buffer ( $\text{NH}_4\text{HCO}_3$  and acetonitrile). The digestion was stopped by addition of formic acid and acetonitrile was removed by vacuum centrifugation. The digested peptides were desalted by zip-tipping (ZipTip pipette tips C18, Millipore). Sequentially, the ZipTip was withdrawn with acetonitrile (wetting solution), and then with water (cleaning solution). The samples were aspirated and retained in the ZipTip, and desalted with formic acid solution following the elution with 50% acetonitrile (ACN). Finally, the samples were dried in vacuum centrifuged and stored in ultrafreezer until the nano-liquid chromatography (nanoLC) and mass spectrometry (MS) analysis.

### nanoLC-Orbitrap mass spectrometry analysis

The digested samples were loaded onto a nanoflow LC (Nano-LC Easy II, Thermo Fisher Scientific, Waltham, MA, USA) connected to a LTQ Orbitrap Velos mass spectrometer (Thermo Fisher Scientific, Waltham, MA, USA). The following columns were used: pre-column Thermo Scientific EASY-Column, C18-A1, 20 × 0.1 mm, particle size 5.0 μm, pore size 120 Å, and analytical column Thermo Scientific EASY-Column, C18-A2, 100 × 0.075 mm, particle size 3.0 μm, pore size 120 Å. The peptides were separated on a 75 min gradient from 2% phase A (99.9% water, 0.1% formic acid) to 45% phase B (95% acetonitrile, 5% water, 0.1% formic acid) in 60 min. In the next 5 min the phase B rises to 95% and remains stable until 10 min in a constant flow rate of 300 nL/min. The spectra was acquired with LTQ-Orbitrap in operation positive ion mode with data-dependent acquisition with full scan ( $m/z$  350 -  $m/z$  1500), an automatic gain control (AGC) target value of 10e6 ions, at maximum fill time of 500 ms at a resolution of 60,000 FWHM followed by 20 MS/MS scans of the most intense ions (> 5000 counts) followed by collision-induced dissociation fragmentation (35% normalized collision energy) with dynamical exclusion of 30 s. The samples

were analyzed in two technical replicates that were combined subsequently to perform the database search.

### Search parameters for NanoLC-Orbitrap

The input data was maximum two missed cleavage sites by trypsin hydrolysis, with the maximum peptide length of 6 and minimum 144. The scoring options were maximum delta Cn 0.05 and max number of peptides reported 10. The mass tolerances were 10 ppm for precursor and 0.05 Da for fragment. The modifications were methionine oxidation (dynamic) and cysteine carbamidomethylation (static). The decoy data base search for target false discovery rate (FDR) was 0.01 (strict) and 0.05 (relaxed).

### Protein identification and Statistic analysis

The proteins were identified by searching in the database NCBIInr (<http://www.ncbi.nlm.nih.gov/protein/>) and Uniprot (<http://www.uniprot.org/>) using the software Proteome Discovery version 1.4 (Thermo Fisher Scientific, Waltham, MA, USA) with the database searching tool SEQUEST (<http://fields.scripps.edu/sequest/>). The identified proteins were quantified using PIAD (Precursor Ion Area Detector) which calculates the areas under the chromatographic peak for those respective identified peptide with resources of the software platform MaxQuant 1.6 [27]. Differentially expressed proteins (DEP) among the comparisons hypothyroidism vs euthyroidism, hypothyroidism vs hyperthyroidism and hyperthyroidism vs euthyroidism were identified with the resources of MSSStats R package and significant differences were considered when adjusted  $p < 0.05$  [28].

### Bioinformatics analysis of identified proteins

The bioinformatics analysis were performed with the significantly altered proteins when compared between the groups using the Cytoscape 3.6.1 software [29]. The Venn diagram and network were constructed using the PINA4MS plug-in to show the unique or shared proteins between the groups [30]. DEP were also used for functional enrichment analysis of Gene Ontology (GO) categories (biological processes, cellular components and molecular function) through ClueGO v2.5.1 + CluePedia v1.5.1 plug-ins [31, 32]. To create the network of biological functions significantly enriched, the following parameters were selected: (1) Analysis mode: functions; (2) Load Marker list: *Rattus Norvegicus*; (3) Visual Style: Groups; (4) ClueGO settings: Biological process + Cellular components + Molecular function; (5) Network Specificity: medium; (6) Use GO term Fusion (only for networks with high

number of terms); (7) Show only Pathways with  $p \leq 0.05$ ; and (8): Kappa Score set to 0.4.

## Results

### Confirmation of thyroid status

The thyroid status was evaluated by the comparison of dehydrated heart weight, TSH and T3 serum concentrations (Table 1). Hypothyroidism induction increased the TSH serum concentration and decreased both T3 serum concentration and the dehydrated heart weight compared to euthyroid animals. In contrast, hyperthyroidism decreased the TSH serum concentrations and increased the dehydrated heart weight compared to euthyroid group.

### Antioxidant enzyme expression and activity in the testis

The *Sod1* transcript expression and SOD activity were not altered by hypo- or hyperthyroidism (Fig. 1a, b). The *Cat* transcript expression and CAT activity were reduced in hypothyroid compared to euthyroid and hyperthyroid rats, while in the hyperthyroid animals these parameters were not altered in comparison with euthyroid animals (Fig. 1c, d). The *Gsr* expression was not altered by hypo- or hyperthyroidism (Fig. 1e), however, hypothyroidism reduced the GSR activity when compared to euthyroidism while no changes were observed in hyperthyroid condition (Fig. 1f). The transcript expression of *Gpx4 var 1* was not altered by hypo or hyperthyroidism (Fig. 1g), while the expression of *Gpx4 var 2* was reduced in the testis of hyperthyroid animals (Fig. 1i). The GPX activity was not different between the experimental groups (Fig. 1h).

### Differentially expressed proteins (DEPs) identified by quantitative proteomic profile of testis by nanoLC-Orbitrap mass spectrometry analysis

All 789 identified proteins and their levels of significance ( $P$  values) were detailed shown in Supplementary Table 2. These proteins are represented in the volcano plot and three comparisons were evaluated: hypothyroidism vs. euthyroidism (Fig. 2a), hyperthyroidism vs. euthyroidism (Fig. 2b) and hypothyroidism vs. hyperthyroidism (Fig. 2c). Compared to the euthyroid group, the hypothyroid group had 337 proteins commonly expressed, in which 123 were downregulated in hypothyroid animals (Fig. 2a and Table 2). Compared to the euthyroid group, the hyperthyroid group had 358 proteins commonly expressed, but none of them was significantly altered (Fig. 2b). Hypo- and hyperthyroidism share 335 proteins commonly expressed, in which

**Table 1** Confirmation of the thyroid status. Data are expressed as mean and standard error of the mean (DHW and T3) or median and interquartile range (TSH)

Group	DHW (mg)	TSH (pg/mL)	T3 (pg/mL)
Euthyroid	337 ± 11 <sup>e</sup>	1,116 [904–1,267] <sup>a</sup>	8,555 ± 513 <sup>a</sup>
Hypothyroid	253 ± 6 <sup>f,g</sup>	12,844 [7,193] <sup>b,g</sup>	6,562 ± 489 <sup>b,g</sup>
Hyperthyroid	396 ± 8 <sup>f,h</sup>	49.6 [39.5–100] <sup>b,h</sup>	9,514 ± 352 <sup>h</sup>

Different letters differ in column: a vs b  $p < 0.05$ , e vs f  $p < 0.001$  and vs h  $p < 0.001$

DHW: dehydrated heart weight

37 were downregulated in hypothyroidism (Fig. 2c and Table 3).

The correlation between the downregulated proteins in Hypothyroid vs. Euthyroid and Hypothyroid vs. Hyperthyroid comparisons is observed in the Venn diagram (Fig. 3a). Thirty-six proteins were downregulated in both comparisons (hypothyroidism vs. euthyroidism and vs. hyperthyroidism), 87 proteins were only downregulated in hypothyroidism vs. euthyroidism and one protein was downregulated exclusively in the hypothyroidism vs. hyperthyroidism comparison (Fig. 3a). The protein–protein interaction resulted in a network with 29 nodes and 68 edges (Fig. 3b), in which a higher number of edges was observed for *Atp5fla*, *Calr*, *Hspa8*, *Park7* and *Uqcrc1* (hypothyroidism vs. euthyroidism and hypothyroidism vs. hyperthyroidism), for *Canx*, *Dld*, *Hsp90b1*, *Hspa5*, *Hspd1*, *Pgam2*, *Sod1*, *Tubb3*, *Tpi1*, *Uqcrc2*, *Vcp* and *Ywhaz* (hypothyroidism vs. euthyroidism) and for *Apoa1* (hypothyroidism vs. hyperthyroidism).

### Functional enrichment analysis of DEPs

The DEPs identified in each comparison were arranged in a functional network according to the most significant GO terms such as biological process, cellular components and molecular function.

The network generated from 123 DEPs from hypothyroidism vs. euthyroidism comparison (Fig. 4 and Supplementary Table 3) revealed a significant enrichment for the following functions: ATP metabolic process (29.17%), coenzyme binding (16.67%), response to temperature stimulus (9.72%), organic hydroxy compound biosynthetic process (8.33%), sperm part (8.33%), peroxiredoxin activity (6.94%), mitochondrial protein complex (4.17), intramolecular oxidoreductase activity (2.78%), binding of sperm to zona pellucida (2.78%), positive regulation of endocytosis (2.78%), ATP biosynthetic process (1.39%), glutathione transferase activity (1.39%), carboxy-lyase activity (1.39%), substantia nigra development (1.39%), negative regulation of protein phosphorylation (1.39%), and melanosome (1.39%).



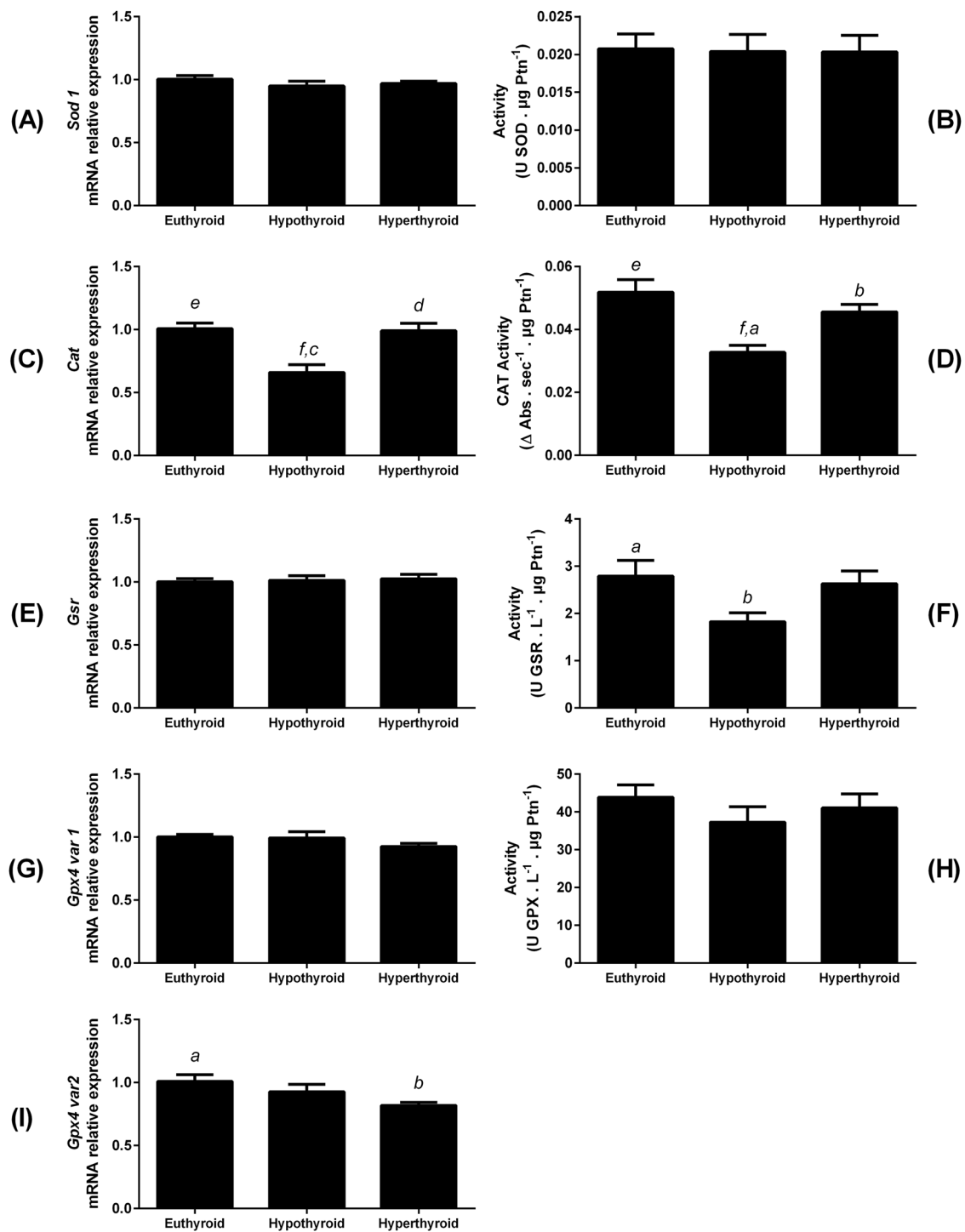


**Fig. 1** Relative transcript expression and activity of antioxidant enzymes in the testis of euthyroid, hypothyroid and hyperthyroid male Wistar rats. **a, b**: Superoxide dismutase, **c, d** Catalase, **e, f** Glutathione reductase and **g–i** Glutathione peroxidase. Data are expressed as mean  $\pm$  S.E.M.; ANOVA followed by Tukey HSD;  $n = 12$ /group; **a** vs. **b**  $P < 0.05$ , **c** vs. **d**  $P < 0.01$ , **e** vs. **f**  $P < 0.001$ . *Sod1*: Superoxide

dismutase 1; SOD: superoxide dismutase; Cat: Catalase; CAT: Catalase; *Gsr*: Glutathione reductase; GSR: Glutathione reductase; *Gpx4var1*: Glutathione peroxidase 4 transcript variant 1; *Gpx4var2*: Glutathione peroxidase 4 transcript variant 2; GPX: Glutathione peroxidase; Abs: absorbance; Ptn: protein

The network generated from 37 DEPs in the hypothyroidism vs. hyperthyroidism comparison (Fig. 5 and Suppl. Table 4) revealed a significant enrichment for the following

functions: binding of sperm to zona pellucida (26.67%), cellular aldehyde metabolic process (26.67%), positive regulation of phagocytosis (13.33%), response to

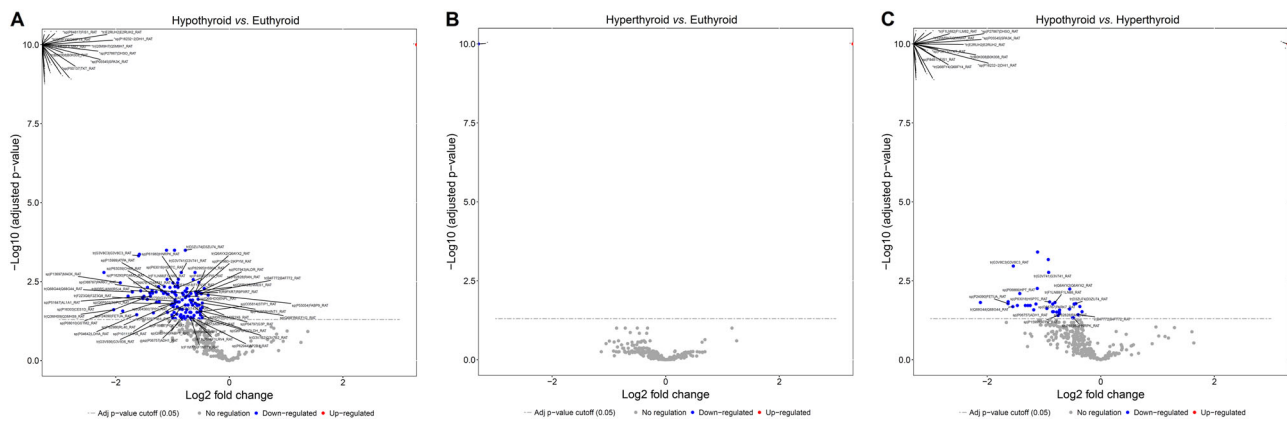


**Fig. 2** Volcano plot of differentially expressed proteins in **a** Hypothyroidism vs Euthyroid, **b** Hyperthyroid vs Euthyroid and **c** Hypothyroid vs Hyperthyroid. In the x-axis is represented the values for  $\text{Log}_2$  fold change and in the y-axis is represented the values for  $-\text{Log}_{10}$

for adjusted  $P$ -value. The dashed line represents the threshold limit (adjusted  $P$ -value = 0.05). The dots represent proteins downregulated in blue, upregulated in red and no regulated in gray

testosterone (6.67%), acute-phase response (6.67%), blood microparticle (6.67%), unfolded protein binding (6.67%), and protein export from nucleus (6.67%).

## Discussion

Imbalances in the antioxidant defense mechanism in the testis are considered the major responsible for the sperm alterations observed in hypo- or hyperthyroid experimental models and men [10–14]. The sperm functionality in animals subjected to hypo- and hyperthyroid presents a reduction in the mitochondrial activity, suggesting an oxidative damage in this organelle [7].

The spermatogenesis process involves intense production of reactive oxygen species (ROS) [33, 34] which is one of the main factor for induction of germ cells apoptosis [34]. The predominant ROS is the superoxide radical ( $\text{O}_2^{\cdot-}$ ) [35], generated mainly from mitochondrial electron transport chain [36] and catalyzed in  $\text{O}_2$  and  $\text{H}_2\text{O}_2$  by the superoxide dismutase (SOD) [37]. The resulting  $\text{H}_2\text{O}_2$  is then metabolized to  $\text{H}_2\text{O}$  and  $\text{O}_2$  by catalase (CAT) or glutathione peroxidase (GPX). Glutathione reductase (GSR) is a NADPH-dependent enzyme responsible for converting the oxidized glutathione (GSSG) molecule to two molecules of reduced glutathione (GSH), maintaining the GSH/GSSG ratio [33, 37, 38]. Taking together the importance of the balance of ROS production and the alterations observed in spermatogenesis in different thyroid conditions, we first investigated the possible alterations induced by hypo- or hyperthyroidism in the testis of adult rats on the transcript expression and activity of the enzymatic antioxidant defense. Hypothyroidism reduced the catalase transcript expression and activity and glutathione reductase activity,

possibly impairing the removal of  $\text{H}_2\text{O}_2$  produced by SOD, which in turn, may contribute for the reduction of sperm acrosome integrity and mitochondrial activity [7]. Hyperthyroidism reduced the content of *Gpx4 var 2* mRNA that encodes the specific sperm nuclei glutathione peroxidase (snGPx). The snGPx is involved in the chromatin condensation during the final stages of spermatogenesis by cross-linked protamine thiols [39]. In this sense, the reduction of *Gpx4 var2* transcript expression in hyperthyroidism could impair the DNA integrity in the chromatin.

Although the impairment on mitochondrial activity was observed in sperm of hypo- and hyperthyroid animals, only hypothyroidism altered the antioxidant enzyme system. To better understand the factors involved in the reproductive dysfunction of hypo- and hyperthyroid animals and to characterize the actions triggered by TH, we have performed a quantitative proteomic profile analysis of adult testes subjected to different thyroid conditions.

Hypothyroidism seems to be more prejudicial to the adult testes physiology since the analysis of differentially expressed proteins revealed that 123 proteins were down-regulated in thyroidectomized rats compared to euthyroid animals, while no significant alterations were observed in testes of animals subjected to T3 challenge during 5 days (hyperthyroid group) compared to euthyroid rats. This testis differential sensitivity to low (hypothyroidism) compared to high (hyperthyroid) levels of thyroid hormones might be due to the period of the treatment performed in our experiments, in which the hypothyroidism was induced by 20 days while the hyperthyroid condition was assessed after 5 days of T3-treatment.

In order to investigate the physiopathological relationship between hypo- and hyperthyroidism the comparison between these two groups was performed. Thirty-six

**Table 2** Down-regulated proteins in hypothyroidism compared to euthyroidism

Gene name	Protein name	Log2 FC	Adj. <i>P</i> value
<i>Aco2</i>	Aconitate hydratase, mitochondrial	−0.8280	0.0242
<i>Acrbp</i>	Acrosin-binding protein	−1.0971	0.0027
<i>Adh1</i>	Alcohol dehydrogenase 1	−0.8256	0.0481
<i>Ahsg</i>	Alpha-2-HS-glycoprotein	−1.2817	0.0142
<i>Akr1a1</i>	Alcohol dehydrogenase [NADP( + )]	−0.9944	0.0034
<i>Akr1b1</i>	Aldose reductase	−0.5694	0.0072
<i>Aldh1a1</i>	Retinal dehydrogenase 1	−1.5041	0.0092
<i>Aldh2</i>	Aldehyde dehydrogenase, mitochondrial	−0.9117	0.0044
<i>Aldh9a1</i>	4-trimethylaminobutyraldehyde dehydrogenase	−0.7791	0.0063
<i>Ap2b1</i>	AP-2 complex subunit beta	−0.6401	0.0450
<i>Asrg1l</i>	Isoaspartyl peptidase/L-asparaginase	−0.5174	0.0298
<i>Ass1</i>	Argininosuccinate synthase	−1.4451	0.0116
<i>Atp5f1a</i>	ATP synthase subunit alpha, mitochondrial	−1.1436	0.0046
<i>Basp1</i>	Brain acid soluble protein 1	−1.0101	0.0361
<i>Cabs1</i>	Calcium-binding and spermatid-specific protein 1	−0.5060	0.0234
<i>Calr</i>	Calreticulin	−0.4425	0.0052
<i>Cand1</i>	Cullin-associated NEDD8-dissociated protein 1	−0.8533	0.0355
<i>Canx</i>	Calnexin	−0.8670	0.0398
<i>Cap1</i>	Adenylyl cyclase-associated protein 1	−1.5824	0.0004
<i>Cct2</i>	T-complex protein 1 subunit beta	−1.3534	0.0074
<i>Cct3</i>	T-complex protein 1 subunit gamma	−1.0049	0.0159
<i>Cct6a</i>	Chaperonin containing Tcp1, subunit 6 A (Zeta 1)	−2.0371	0.0246
<i>Cct7</i>	Chaperonin-containing TCP1 subunit 7	−1.4426	0.0049
<i>Cct8</i>	Chaperonin containing TCP1 subunit 8	−0.8097	0.0082
<i>Ces1d</i>	Carboxylesterase 1D	−1.3887	0.0091
<i>Cfap36</i>	Cilia- and flagella-associated protein 36	−0.9663	0.0003
<i>Cltc</i>	Clathrin heavy chain	−0.6823	0.0455
<i>Cnbp</i>	Cellular nucleic acid-binding protein	−0.6758	0.0075
<i>Creld2</i>	Cysteine-rich with EGF-like domain protein 2	−0.8291	0.0119
<i>Cs</i>	Citrate synthase	−0.9243	0.0340
<i>Dbil5</i>	Diazepam-binding inhibitor-like 5	−0.5258	0.0298
<i>Ddt</i>	D-dopachrome decarboxylase	−0.6215	0.0372
<i>Dld</i>	Dihydropyridyl dehydrogenase, mitochondrial	−0.5080	0.0360
<i>Dnpep</i>	Aspartyl aminopeptidase	−1.5282	0.0102
<i>Dync1i2</i>	Cytoplasmic dynein 1 intermediate chain 2	−0.7743	0.0003
<i>Eef1g</i>	Elongation factor 1-gamma	−0.4752	0.0151
<i>Eef2</i>	Elongation factor 2	−1.1924	0.0062
<i>Eno1-ps1</i>	Enolase 1, (alpha), pseudogene 1	−1.2906	0.0068
<i>Fabp9</i>	Fatty acid-binding protein 9	−0.4945	0.0077
<i>Gapdh</i>	Glyceraldehyde-3-phosphate dehydrogenase	−0.5000	0.0270
<i>Gdi2</i>	Rab GDP dissociation inhibitor beta	−0.6020	0.0154
<i>Gkap1</i>	G kinase-anchoring protein 1	−0.3725	0.0085
<i>Glul</i>	Glutamine synthetase	−1.1066	0.0003
<i>Gstm2</i>	Glutathione S-transferase Mu 2	−1.5233	0.0109
<i>Gstm5</i>	Glutathione S-transferase Mu 5	−1.0463	0.0049
<i>Gstm6</i>	Glutathione S-transferase	−1.8780	0.0270
<i>Hadha</i>	Trifunctional enzyme subunit alpha, mitochondrial	−1.5612	0.0062
<i>Hadhb</i>	Trifunctional enzyme subunit beta, mitochondrial	−0.9731	0.0298
<i>Hint1</i>	Histidine triad nucleotide-binding protein 1	−0.5497	0.0114
<i>Hmgcs2</i>	3-hydroxy-3-methylglutaryl coenzyme A synthase	−1.7069	0.0068
<i>Hnrnpk</i>	Heterogeneous nuclear ribonucleoprotein K	−0.8974	0.0027
<i>Hp</i>	Haptoglobin	−0.7348	0.0400
<i>Hsp90aa1</i>	Heat shock protein HSP 90-alpha	−0.5949	0.0068
<i>Hsp90b1</i>	Endoplasmic	−0.7104	0.0090
<i>Hspa1l</i>	Heat shock 70 kDa protein 1-like	−0.5686	0.0180
<i>Hspa2</i>	Heat shock-related 70 kDa protein 2	−0.6364	0.0027



**Table 2** (continued)

Gene name	Protein name	Log2 FC	Adj. <i>P</i> value
<i>Hspa4</i>	Heat shock 70 kDa protein 4	−0.6771	0.0428
<i>Hspa4l</i>	Heat shock 70 kDa protein 4-like	−0.4870	0.0075
<i>Hspa5</i>	Endoplasmic reticulum chaperone BiP	−0.5346	0.0068
<i>Hspa8</i>	Heat shock cognate 71 kDa protein	−0.9568	0.0046
<i>Hspd1</i>	60 kDa heat shock protein, mitochondrial	−1.1305	0.0069
<i>Hyou1</i>	Hyou1 protein	−0.7756	0.0102
<i>Ipo4</i>	Importin 4	−1.3590	0.0061
<i>Ipo5</i>	Importin 5	−0.9556	0.0119
<i>Isyna1</i>	Inositol-3-phosphate synthase 1	−0.8832	0.0139
<i>Kpnb1</i>	Importin subunit beta-1	−0.9466	0.0132
<i>Ldha</i>	L-lactate dehydrogenase A chain	−1.6315	0.0354
<i>Ldhb</i>	L-lactate dehydrogenase B chain	−1.3378	0.0309
<i>Ldhc</i>	L-lactate dehydrogenase	−0.5365	0.0033
<i>Lgals1</i>	Galectin-1	−0.7497	0.0246
<i>LOC100360413</i>	Elongation factor 1-alpha	−0.6496	0.0175
<i>LOC102556347</i>	Carbonyl reductase [NADPH] 1-like	−0.6903	0.0122
<i>Lrrc46</i>	Leucine rich repeat containing 46	−0.4787	0.0441
<i>Marcks1l</i>	MARCKS-related protein	−0.9548	0.0068
<i>Me1</i>	NADP-dependent malic enzyme	−1.9207	0.0034
<i>Nasp</i>	Nuclear autoantigenic sperm protein	−0.7476	0.0052
<i>Nmes1</i>	Normal mucosa of esophagus-specific gene 1 protein	−0.7536	0.0068
<i>Nrdc</i>	Nardilysin	−0.7503	0.0090
<i>Nsfl1c</i>	NSFL1 cofactor p47	−0.5347	0.0479
<i>P4hb</i>	Protein disulfide-isomerase	−0.9994	0.0449
<i>Pabpc1</i>	Polyadenylate-binding protein 1	−0.8465	0.0433
<i>Park7</i>	Protein/nucleic acid deglycase DJ-1	−0.8223	0.0074
<i>Pdia6</i>	Protein disulfide-isomerase A6	−1.0784	0.0079
<i>Pdilt</i>	Protein disulfide-isomerase-like protein of the testis	−2.2093	0.0016
<i>Pebp1</i>	Phosphatidylethanolamine-binding protein 1	−0.6054	0.0016
<i>Pgam2</i>	Phosphoglycerate mutase 2	−1.3973	0.0074
<i>Pgk1</i>	Phosphoglycerate kinase 1	−0.8729	0.0234
<i>Pgk2</i>	Phosphoglycerate kinase	−0.7280	0.0175
<i>Pgp</i>	Glycerol-3-phosphate phosphatase	−0.6769	0.0298
<i>Pkm</i>	Pyruvate kinase	−0.5833	0.0068
<i>Ppia</i>	Peptidyl-prolyl cis-trans isomerase A	−0.9838	0.0198
<i>Ppt1</i>	Palmitoyl-protein thioesterase 1	−0.6955	0.0296
<i>Prdx1</i>	Peroxiredoxin-1	−0.6695	0.0145
<i>Prdx4</i>	Peroxiredoxin-4	−0.9113	0.0034
<i>Ptges3</i>	Prostaglandin E synthase 3	−0.5851	0.0074
<i>Ptpa</i>	Serine/threonine-protein phosphatase 2 A activator	−0.9611	0.0075
<i>Ran</i>	GTP-binding nuclear protein Ran	−0.5779	0.0085
<i>Rida</i>	2-iminobutanoate/2-iminopropanoate deaminase	−1.0939	0.0079
<i>Rpn2</i>	Dolichyl-diphosphooligosaccharide-protein glycosyltransferase subunit 2	−0.9178	0.0200
<i>Serpina1</i>	Alpha-1-antitrypsin	−1.7836	0.0092
<i>Shcbl1</i>	SHC-binding and spindle-associated 1-like	−0.8004	0.0398
<i>Slc25a3</i>	Phosphate carrier protein, mitochondrial	−0.8469	0.0016
<i>Smcp</i>	Sperm mitochondrial-associated cysteine-rich protein	−0.7736	0.0479
<i>Sod1</i>	Superoxide dismutase [Cu-Zn]	−0.5345	0.0175
<i>Spa17</i>	Sperm surface protein Sp17	−1.2458	0.0046
<i>Stip1</i>	Stress-induced-phosphoprotein 1	−0.5701	0.0296
<i>Sugt1</i>	Protein SGT1 homolog	−1.0085	0.0068
<i>Tcp1</i>	T-complex protein 1 subunit alpha	−0.9525	0.0466
<i>Tcp11</i>	T-complex protein 11 homolog	−0.9393	0.0085
<i>Tkfc</i>	Triokinase/FMN cyclase	−1.0256	0.0175
<i>Tmsb4x</i>	Thymosin beta-4	−0.7755	0.0175
<i>Tpi1</i>	Triosephosphate isomerase	−0.9036	0.0049

**Table 2** (continued)

Gene name	Protein name	Log2 FC	Adj. <i>P</i> value
<i>Tpp2</i>	Tripeptidyl-peptidase 2	−0.9038	0.0139
<i>Tubb3</i>	Tubulin beta-3 chain	−1.1597	0.0075
<i>Uba1</i>	Ubiquitin-like modifier-activating enzyme 1	−1.0899	0.0298
<i>Uba52</i>	Ubiquitin-60S ribosomal protein L40	−0.9558	0.0147
<i>Uqcrc1</i>	Cytochrome b-c1 complex subunit 1, mitochondrial	−0.4789	0.0209
<i>Uqcrc2</i>	Cytochrome b-c1 complex subunit 2, mitochondrial	−0.9665	0.0159
<i>Vcp</i>	Transitional endoplasmic reticulum ATPase	−1.2351	0.0139
<i>Vim</i>	Vimentin	−1.5974	0.0005
<i>Ywhae</i>	14–3–3 protein epsilon	−0.6471	0.0121
<i>Ywhaq</i>	14–3–3 protein theta	−0.7677	0.0298
<i>Ywhaz</i>	14–3–3 protein zeta/delta	−0.6691	0.0490

*FC* fold change, *Adj.* Adjusted

**Table 3** Downregulated proteins in hypothyroidism compared to hyperthyroidism

Gene name	Protein name	Log2 FC	Adj. <i>P</i> value
<i>Acrbp</i>	Acrosin-binding protein	−0.8471	0.0171
<i>Adh1</i>	Alcohol dehydrogenase 1	−1.1809	0.0262
<i>Ahsg</i>	Alpha-2-HS-glycoprotein	−1.6326	0.0166
<i>Akr1a1</i>	Alcohol dehydrogenase [NADP( + )]	−0.7299	0.0301
<i>Aldh2</i>	Aldehyde dehydrogenase, mitochondrial	−0.8063	0.0153
<i>Apoa1</i>	Apolipoprotein A-I	−1.2840	0.0191
<i>Atp5f1a</i>	ATP synthase subunit alpha, mitochondrial	−0.7521	0.0395
<i>Calr</i>	Calreticulin	−0.3679	0.0207
<i>Cap1</i>	Adenylyl cyclase-associated protein 1	−1.1182	0.0055
<i>Cct2</i>	T-complex protein 1 subunit beta	−1.3278	0.0191
<i>Cct7</i>	Chaperonin-containing TCP1 subunit 7	−1.2421	0.0191
<i>Cfap36</i>	Cilia- and flagella-associated protein 36	−0.9239	0.0007
<i>Dync1i2</i>	Cytoplasmic dynein 1 intermediate chain 2	−0.4392	0.0166
<i>Glul</i>	Glutamine synthetase	−1.1136	0.0004
<i>Gstm5</i>	Glutathione S-transferase Mu 5	−0.7278	0.0338
<i>Hadha</i>	Trifunctional enzyme subunit alpha, mitochondrial	−1.6306	0.0145
<i>Hmgcs2</i>	3-hydroxy-3-methylglutaryl coenzyme A synthase	−1.5480	0.0208
<i>Hnrnpk</i>	Heterogeneous nuclear ribonucleoprotein K	−0.4802	0.0470
<i>Hp</i>	Haptoglobin	−1.4264	0.0080
<i>Hspa2</i>	Heat shock-related 70 kDa protein 2	−0.4686	0.0171
<i>Hspa4l</i>	Heat shock 70 kDa protein 4-like	−0.3976	0.0374
<i>Hspa8</i>	Heat shock cognate 71 kDa protein	−0.9012	0.0147
<i>Ldhc</i>	L-lactate dehydrogenase	−0.5472	0.0057
<i>Nasp</i>	Nuclear autoantigenic sperm protein	−0.4968	0.0470
<i>Park7</i>	Protein/nucleic acid deglycase DJ-1	−0.7256	0.0265
<i>Pdia6</i>	Protein disulfide-isomerase A6	−1.1415	0.0171
<i>Pdilt</i>	Protein disulfide-isomerase-like protein of the testis	−1.4681	0.0191
<i>Pebp1</i>	Phosphatidylethanolamine-binding protein 1	−0.3302	0.0301
<i>Ptpa</i>	Serine/threonine-protein phosphatase 2 A activator	−0.8336	0.0301
<i>Ran</i>	GTP-binding nuclear protein Ran	−0.5499	0.0247
<i>Serpinal1</i>	Alpha-1-antiproteinase	−2.1189	0.0153
<i>Slc25a3</i>	Phosphate carrier protein, mitochondrial	−0.9179	0.0017
<i>Spa17</i>	Sperm surface protein Sp17	−0.9485	0.0238
<i>Sugt1</i>	Protein SGT1 homolog	−0.7767	0.0310
<i>Tcp11</i>	T-complex protein 11 homolog	−0.8474	0.0301
<i>Uqcrc1</i>	Cytochrome b-c1 complex subunit 1, mitochondrial	−0.4849	0.0470
<i>Vim</i>	Vimentin	−1.5397	0.0011

*FC* fold change, *Adj.* Adjusted

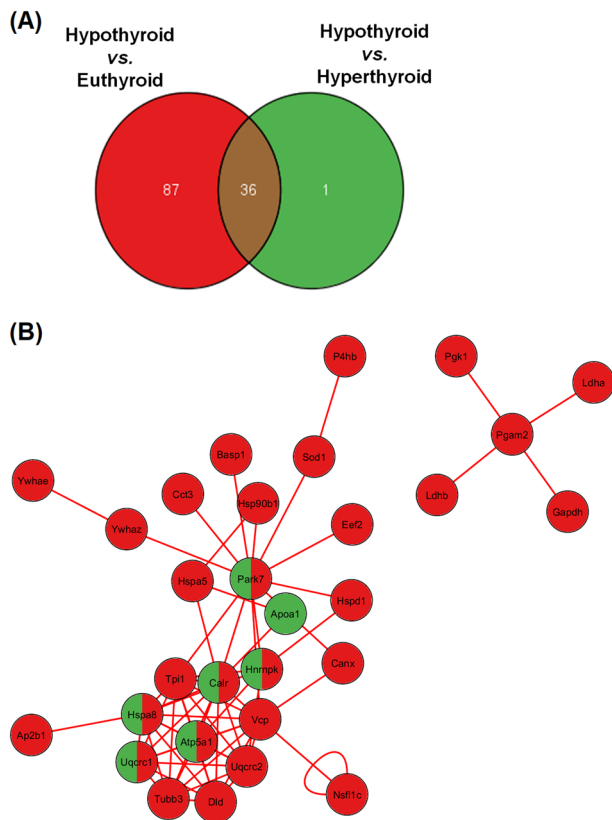


**Fig. 3** **a** Venn diagram of down-regulated proteins unique or shared between hypothyroid vs euthyroid and hyperthyroid vs hypothyroid. A total 36 shared down-regulated proteins in both comparisons, 87 expressed proteins only in the hypothyroid vs euthyroid comparison, and a single expressed protein in the hyperthyroid vs hypothyroid comparison. **b** Visual representation of protein–protein interaction network of downregulated proteins in the comparisons hypothyroid vs euthyroid (red nodes) and hyperthyroid vs hypothyroid (green nodes) groups. The bicolor nodes (green and red) are in common for both comparisons

proteins were downregulated in both hypo-euthyroid and hypo-hyperthyroid comparisons, 87 proteins were down-regulated in hypo-euthyroid comparison, while one protein (APOA1) was reduced only in hypo-hyperthyroid comparison. These data suggest that the regulation at molecular level, resulting in differential protein expression profile in adult testes, could explain the distinct clinical features observed in men reproductive pathological-induced condition, as hypo- or hyperthyroidism.

The analysis of protein–protein interaction shows that some protein, such as *Atp5f1a*, *Calr*, *Hspa8*, and *Park7* are reduced in both hypo-euthyroid and hypo-hyperthyroid comparisons. These proteins are involved in several cellular processes, evidenced by the greater number of nodes, in which each node represents a common pathway for particular cell function [40].

Regarding the functional role of the proteins mentioned above, the mitochondrial membrane ATP synthase

(*Atp5f1a*) is an important enzyme that produces ATP from ADP in the presence of a proton gradient across generated by the electron transport complexes of the respiratory chain [41]. The generation of energy is primordial to maintain the high rates of cell division during spermatogenesis process [9]. *Calr* is a calcium-binding chaperone that interact with newly synthesized glycoproteins, regulating the calcium homeostasis and the process of protein maturation and degradation [42]. In the testis, *Calr* is present in the acrosome of spermatids [43], interfering with the protein *Adam3* during spermatogenesis [44] which will affect the sperm motility and acrosome reaction [45], with negative effects in the sperm fertilizing ability. *Hspa8* is a chaperone, member of the hsp70 protein, which plays indispensable roles during sperm development being associated with acrosome biogenesis, chromatin compaction, DNA packaging, sperm capacitation [42]. Disruption in its function causes reduction in sperm count and motility, abnormal sperm morphology impaired DNA condensation [42]. *Park7*, also known as sperm membrane protein 22, was identified in the proteomic characterization of the human sperm nucleus [46] and plays a role in both the zona penetration and membrane fusion steps of fertilization [47]. Besides, *Park7* may cooperate with *SOD1* in the oxidative stress response pathway [48]. *Park7* was also addressed to impair mitochondrial activity in sperm contributing to asthenozoospermia (reduced sperm motility) pathogenesis in men [49].

The functional enrichment analysis of hypo-euthyroid comparison also pointed out for peroxiredoxin activity and cellular oxidant detoxification terms, in which the peroxiredoxins 1 (*Prxd1*) and 4 (*Prxd4*) are involved. *Prdxs* are selenium-free enzymes highly reactive with  $H_2O_2$  and other peroxides and are involved in the protection of human spermatozoa against the oxidative stress [50, 51]. The animals knocked out for *Prxd4* present loss of spermatogenic cells and increase of apoptosis in the testis [50] while reduction in the *Prxd1* is associated to increased levels of sperm lipid peroxidation, DNA damage and impairment of sperm motility [51].

The reduction of *Apoa1* protein content was observed exclusively in hypo-hyperthyroid comparison. *Apoa1* is located in the cellular membrane of testis and participates of cholesterol influx for the steroidogenesis process [52]. It was also identified as an activator of sperm motility [53].

Some proteins involved in the glycolytic pathway and energy production, such as *Ldhc*, *Gapdh*, *Pgk2* and *Tpi1* were reduced in the hypo-euthyroid comparison and were grouped in ATP metabolic process pathways and ATP biosynthetic process terms. They are important for the energy production from glycolysis in spermatid cells [54–57]. Interestingly, during sperm development and maturation there is a switch regarding the main source of

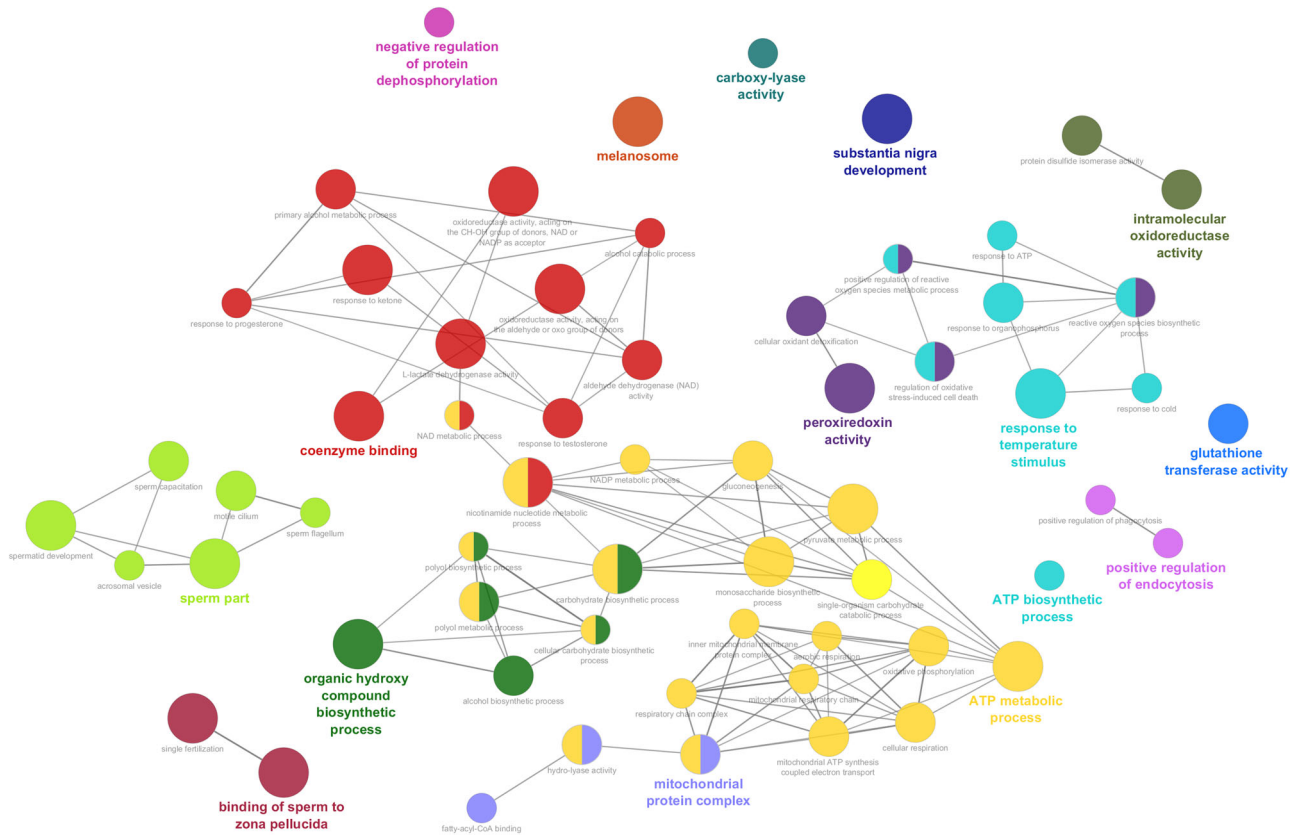


**Fig. 4** Visual representation of Gene Ontology enrichment analysis of 123 downregulated proteins in hypothyroid vs. euthyroid comparison. The identified proteins were grouped into a network of function and related processes of non-redundant biological terms. The nodes of

similar biological terms were represented with the same color and their sizes reflect their significance. The most significant pathway of each group has a highlighted label. All analyses were performed using the Cytoscape ClueGO plus CluePedia plug-ins,  $p < 0.05$

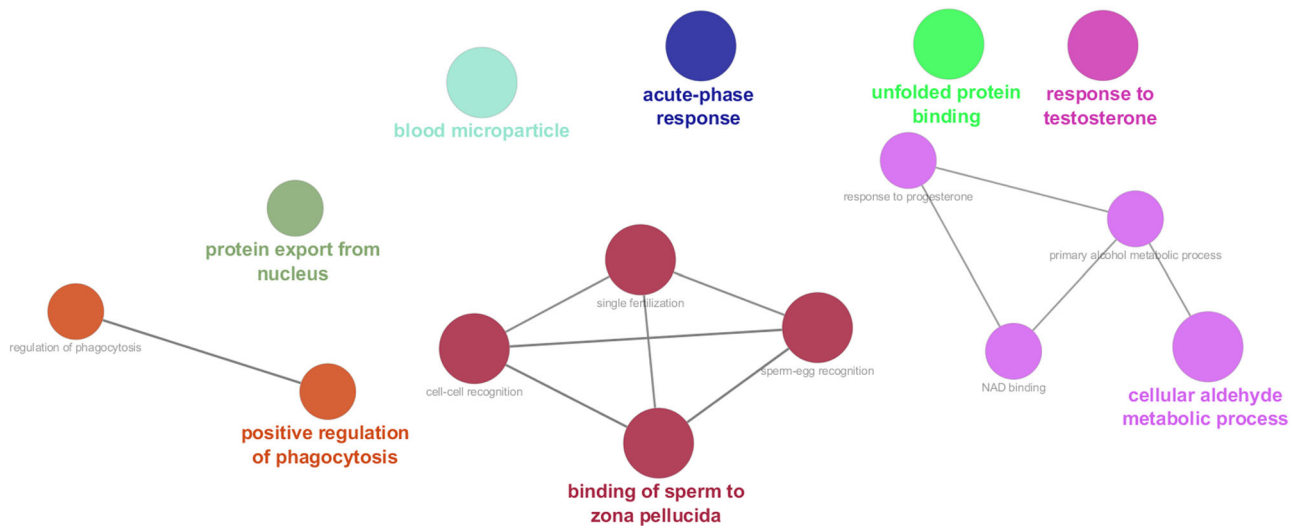


**Fig. 5** Visual representation of Gene Ontology enrichment analysis of 37 downregulated proteins in hypothyroid vs. hyperthyroid comparison. The identified proteins were grouped into a network of function and related processes of non-redundant biological terms. The nodes of

similar biological terms were represented with the same color and their sizes reflect their significance. The most significant pathway of each group has a highlighted label. All analyses were performed using the Cytoscape ClueGO plus CluePedia plug-ins,  $p < 0.05$

ATP. In the initial steps the main source of ATP is the oxidative phosphorylation [58] and during sperm maturation is the glycolysis [59]. In association with the fibrous sheath, these enzymes form a specialized metabolosome within the sperm flagellum, which is responsible for generating ATP in this cell that has scarce cytoplasm [56]. Thus, the reduction in energy production due to decrease in glycolysis affect the sperm maturation, impairing the spermatic motility and fertilizing ability.

It is important to mention that quantitative proteome identifies differentially expressed proteins based on the statistical methods developed for large scale experiments (high throughput method), and consequently, slightly alterations in some proteins could failed to be recognized by this method. Another aspect to consider is that the trypsin digestion of the sample may generates small peptides fragments that lack in the protein identity. Therefore, low throughput methods for protein quantification (based by antibody detection) may eventually discover another altered proteins not presented in this study. Thus, further validation is required to confirm the results and the interactions between the different thyroid conditions obtained by quantitative proteome analysis.

In summary, hypothyroidism developed in adulthood reduces the activity of antioxidant defense mechanism in testis of rats, probably increasing the ROS production resulting in reduced sperm functionality, mitochondrial activity and acrosome integrity. Moreover, the expression of several proteins involved in the metabolism of spermatid cells, binding of sperm to zona pellucida, among others, is potentially affected in hypothyroidism. All these alterations point out a complex correlation between reproductive dysfunctions, as infertility, and thyroid disorders which may correlate with the signs obtained from hypothyroid patients in clinical studies.

**Acknowledgements** We thank the Core Facility for Scientific Research – University of Sao Paulo (CEFAP-USP/BIOMASS) for the mass spectrometry analysis.

**Funding** This study was funded by the Fundação de Amparo à Pesquisa do Estado de São Paulo – FAPESP (2014/10845–0), Conselho Nacional de Desenvolvimento Científico e Tecnológico - CNPq (164380/2014–0 and 305509/2013–6), Coordenação de Aperfeiçoamento de Pessoal de Nível Superior – Brasil (CAPES) (Finance Code 001) and Fundação Araucária, Brazil.

## Compliance with ethical standards

**Conflict of interest** The authors declare that they have no conflict of interest.

**Ethical approval** All applicable international, national, and/or institutional guidelines for the care and use of animals were followed and approved by the Universidade Estadual do Centro-Oeste, Ethical Committee for Animal Research (protocol # CEUA 010/2014).

**Publisher's note:** Springer Nature remains neutral with regard to jurisdictional claims in published maps and institutional affiliations.

## References

1. M. Vander Borgh, C. Wyns, Fertility and infertility: definition and epidemiology. *Clin. Biochem.* **62**, 9 (2018). <https://doi.org/10.1016/j.clinbiochem.2018.03.012>
2. M. Punab, O. Poolamets, P. Paju, V. Vihljajev, K. Pomm, R. Ladva, P. Korrovits, M. Laan, Causes of male infertility: a 9-year prospective monocentre study on 1737 patients with reduced total sperm counts. *Hum. Reprod.* **32**, 18–31 (2017). <https://doi.org/10.1093/humrep/dew284>
3. S. La Vignera, R. Vita, Thyroid dysfunction and semen quality. *Int. J. Immunopathol. Pharmacol.* **32**, 2058738418775241 (2018). <https://doi.org/10.1177/2058738418775241>
4. S. La Vignera, R. Vita, R.A. Condorelli, L.M. Mongioì, S. Presti, S. Benvenga, A.E. Calogero, Impact of thyroid disease on testicular function. *Endocrine* 1–11 (2017). <https://doi.org/10.1007/s12020-017-1303-8>
5. P.N. Taylor, D. Albrecht, A. Scholz, G. Gutierrez-Buey, J.H. Lazarus, C.M. Dayan, O.E. Okosieme, Global epidemiology of hyperthyroidism and hypothyroidism. *Nat. Rev. Endocrinol.* **14**, 301–316 (2018). <https://doi.org/10.1038/nrendo.2018.18>
6. F. Lotti, E. Maseroli, N. Fralassi, S. Degl'Innocenti, L. Boni, E. Baldi, M. Maggi, Is thyroid hormones evaluation of clinical value in the work-up of males of infertile couples? *Hum. Reprod.* **31**, 518–529 (2016). <https://doi.org/10.1093/humrep/dev338>
7. R.M. Romano, S.N. Gomes, N.C. Cardoso, L. Schiessl, M.A. Romano, C.A. Oliveira, New insights for male infertility revealed by alterations in spermatid function and differential testicular expression of thyroid-related genes. *Endocrine* **55**, 607–617 (2017). <https://doi.org/10.1007/s12020-016-0952-3>
8. M.E. Martinez, A. Karaczyn, J.P. Stohn, W.T. Donnelly, W. Croteau, R.P. Peeters, V.A. Galton, D., St Forrest, D. Germain, A. Hernandez, The type 3 deiodinase is a critical determinant of appropriate thyroid hormone action in the developing testis. *Endocrinology* **157**, 1276–1288 (2016). <https://doi.org/10.1210/en.2015-1910>
9. R.J. Aitken, Z. Gibb, M.A. Baker, J. Drevet, P. Gharagozloo, Causes and consequences of oxidative stress in spermatozoa. *Reprod. Fertil. Dev.* **28**, 1–10 (2016)
10. S. Chattopadhyay, S. Choudhury, A. Roy, G.B.N. Chainy, L. Samanta, T3 fails to restore mitochondrial thiol redox status altered by experimental hypothyroidism in rat testis. *Gen. Comp. Endocrinol.* **169**, 39–47 (2010). <https://doi.org/10.1016/j.ygcen.2010.07.014>
11. D.K. Sahoo, A. Roy, S. Bhanja, G.B. Chainy, Hypothyroidism impairs antioxidant defence system and testicular physiology during development and maturation. *Gen. Comp. Endocrinol.* **156**, 63–70 (2008). <https://doi.org/10.1016/j.ygcen.2007.11.007>
12. D.K. Sahoo, A. Roy, Compromised rat testicular antioxidant defence system by hypothyroidism before puberty. *Int. J. Endocrinol.* **2012**, 11 (2012). <https://doi.org/10.1155/2012/637825>
13. A.R. Chowdhury, A.K. Gautam, B.B. Chatterjee, Thyroid-testis interrelationship during the development and sexual maturity of the rat. *Arch. Androl.* **13**, 233–239 (1984). <https://doi.org/10.3109/01485018408987522>
14. S. Nazeri, M. Rostamian, M. Hedayati, Impact of thyroid dysfunction on antioxidant capacity, superoxide dismutase and catalase activity. *J. Res. Med. Sci.* **16**, 51–54 (2014)
15. P. Vernet, R.J. Aitken, J.R. Drevet, Antioxidant strategies in the epididymis. *Mol. Cell. Endocrinol.* **216**, 31–39 (2004). <https://doi.org/10.1016/j.mce.2003.10.069>



16. C. Huang, X. Cao, D. Pang, C. Li, Q. Luo, Y. Zou, B. Feng, L. Li, A. Cheng, Z. Chen, Is male infertility associated with increased oxidative stress in seminal plasma? A-meta analysis. *Oncotarget* **9**, 24494–24513 (2018). <https://doi.org/10.18632/oncotarget.25075>
17. A.G. Cicatiello, D. Di Girolamo, M. Dentice, Metabolic effects of the intracellular regulation of thyroid hormone: old players, new concepts. *Front Endocrinol.* **9**, 474 (2018). <https://doi.org/10.3389/fendo.2018.00474>
18. A.C. Bianco, G. Anderson, D. Forrest, V.A. Galton, B. Gereben, B.W. Kim, P.A. Kopp, X.H. Liao, M.J. Obregon, R.P. Peeters, S. Refetoff, D.S. Sharlin, W.S. Simonides, R.E. Weiss, G.R. Williams, American Thyroid Association Task Force on, A., Strategies to Investigate Thyroid Hormone, E., Action: American Thyroid Association Guide to investigating thyroid hormone economy and action in rodent and cell models. *Thyroid* **24**, 88–168 (2014). <https://doi.org/10.1089/thy.2013.0109>
19. P. Bargi-Souza, R.M. Romano, M. Salgado Rde, F. Goulart-Silva, E.L. Brunetto, T.M. Zorn, M.T. Nunes, Triiodothyronine rapidly alters the TSH content and the secretory granules distribution in male rat thyrotrophs by a cytoskeleton rearrangement-independent mechanism. *Endocrinology* **154**, 4908–4918 (2013). <https://doi.org/10.1210/en.2013-1508>
20. K.J. Livak, T.D. Schmittgen, Analysis of relative gene expression data using real-time quantitative PCR and the 2(-Delta Delta C(T)) Method. *Methods* **25**, 402–408 (2001). <https://doi.org/10.1006/meth.2001.1262>
21. M.M. Bradford, A rapid and sensitive method for the quantitation of microgram quantities of protein utilizing the principle of protein-dye binding. *Anal. Biochem.* **72**, 248–254 (1976). [https://doi.org/10.1016/0003-2697\(76\)90527-3](https://doi.org/10.1016/0003-2697(76)90527-3)
22. C. Beauchamp, I. Fridovich, Superoxide dismutase: Improved assays and an assay applicable to acrylamide gels. *Anal. Biochem.* **44**, 276–287 (1971). [https://doi.org/10.1016/0003-2697\(71\)90370-8](https://doi.org/10.1016/0003-2697(71)90370-8)
23. D.E. Paglia, W.N. Valentine, Studies on the quantitative and qualitative characterization of erythrocyte glutathione peroxidase. *J. Lab. Clin. Med.* **70**, 158–169 (1967). <https://doi.org/10.5555/uri:pii:0022214367900765>
24. K.G. Melissinos, A.Z. Delidou, A.G. Varsou, S.S. Begietti, G.J. Drivas, Serum and erythrocyte glutathione reductase activity in chronic renal failure. *Nephron.* **28**, 76–79 (1981)
25. J.T. Rotruck, A.L. Pope, H.E. Ganther, A.B. Swanson, D.G. Hafeman, W.G. Hoekstra, Selenium: biochemical role as a component of glutathione peroxidase. *Science* **179**, 588–590 (1973)
26. H. Aebi, [13] Catalase in vitro. In: *Methods in Enzymology*, vol. 105. (Academic Press, Massachusetts, USA, 1984), pp. 121–126
27. J. Cox, M. Mann, MaxQuant enables high peptide identification rates, individualized p.p.b.-range mass accuracies and proteome-wide protein quantification. *Nat. Biotechnol.* **26**, 1367 (2008). <https://doi.org/10.1038/nbt.1511>
28. M. Choi, C.Y. Chang, T. Clough, D. Broudy, T. Killeen, B. MacLean, O. Vitek, MSstats: an R package for statistical analysis of quantitative mass spectrometry-based proteomic experiments. *Bioinformatics* **30**, 2524–2526 (2014). <https://doi.org/10.1093/bioinformatics/btu305>
29. P. Shannon, A. Markiel, O. Ozier, N.S. Baliga, J.T. Wang, D. Ramage, N. Amin, B. Schwikowski, T. Ideker, Cytoscape: a software environment for integrated models of biomolecular interaction networks. *Genome Res.* **13**, 2498–2504 (2003). <https://doi.org/10.1101/gr.1239303>
30. J. Wu, T. Vollenius, K. Ovaska, J. Westermark, T.P. Makela, S. Hautaniemi, Integrated network analysis platform for protein-protein interactions. *Nat. Methods* **6**, 75–77 (2009). <https://doi.org/10.1038/nmeth.1282>
31. G. Bindea, J. Galon, B. Mlecnik, CluePedia Cytoscape plugin: pathway insights using integrated experimental and in silico data. *Bioinformatics* **29**, 661–663 (2013). <https://doi.org/10.1093/bioinformatics/btt019>
32. G. Bindea, B. Mlecnik, H. Hackl, P. Charoentong, M. Tosolini, A. Kirilovsky, W.H. Fridman, F. Pages, Z. Trajanoski, J. Galon, ClueGO: a Cytoscape plug-in to decipher functionally grouped gene ontology and pathway annotation networks. *Bioinformatics* **25**, 1091–1093 (2009). <https://doi.org/10.1093/bioinformatics/btp101>
33. G. Guerriero, S. Trocchia, F.K. Abdel-Gawad, G. Ciarcia, Roles of reactive oxygen species in the spermatogenesis regulation. *Front. Endocrinol.* **5**, 1–4 (2014).
34. Y.-R. Xu, H.-S. Dong, W.-X. Yang, Regulators in the apoptotic pathway during spermatogenesis: Killers or guards? *Gene* **582**, 97–111 (2016). <https://doi.org/10.1016/j.gene.2016.02.007>
35. R.R. Henkel, Leukocytes and oxidative stress: dilemma for sperm function and male fertility. *Asian J. Androl.* **13**, 43–52 (2011). <https://doi.org/10.1038/aja.2010.76>
36. R.J. Aitken, S.D. Roman, Antioxidant systems and oxidative stress in the testes. *Oxid. Med. Cell Longev.* **1**, 15–24 (2008)
37. F. Bauche, M.H. Fouchard, B. Jegou, Antioxidant system in rat testicular cells. *FEBS Lett.* **349**, 392–396 (1994)
38. W.Y. Wong, C.M. Thomas, J.M. Merkus, G.A. Zielhuis, R.P. Steegers-Theunissen, Male factor subfertility: possible causes and the impact of nutritional factors. *Fertil. Steril.* **73**, 435–442 (2000)
39. H. Pfeifer, M. Conrad, D. Roethlein, A. Kyriakopoulos, M. Brielmeier, G.W. Bornkamm, D. Behne, Identification of a specific sperm nuclei selenoenzyme necessary for protamine thiol cross-linking during sperm maturation. *FASEB J.* **15**, 1236–1238 (2001)
40. G. Bebek, Identifying gene interaction networks. *Methods Mol. Biol.* **850**, 483–494 (2012). [https://doi.org/10.1007/978-1-61779-555-8\\_26](https://doi.org/10.1007/978-1-61779-555-8_26)
41. A.I. Jonckheere, J.A.M. Smeitink, R.J.T. Rodenburg, Mitochondrial ATP synthase: architecture, function and pathology. *J. Inher. Metab. Dis.* **35**, 211–225 (2012). <https://doi.org/10.1007/s10545-011-9382-9>
42. M.D. Dun, R.J. Aitken, B. Nixon, The role of molecular chaperones in spermatogenesis and the post-testicular maturation of mammalian spermatozoa. *Hum. Reprod. Update* **18**, 420–435 (2012). <https://doi.org/10.1093/humupd/dms009>
43. M. Nakamura, Y. Michikawa, T. Baba, S. Okinaga, K. Arai, Calreticulin is present in the acrosome of spermatids of rat testis. *Biochem. Biophys. Res. Commun.* **186**, 668–673 (1992)
44. M. Ikawa, K. Tokuhira, R. Yamaguchi, A.M. Benham, T. Tamura, I. Wada, Y. Satouh, N. Inoue, M. Okabe, Calsperin is a testis-specific chaperone required for sperm fertility. *J. Biol. Chem.* **286**, 5639–5646 (2011). <https://doi.org/10.1074/jbc.M110.140152>
45. M. Nakamura, M. Moriya, T. Baba, Y. Michikawa, T. Yamanobe, K. Arai, S. Okinaga, T. Kobayashi, An endoplasmic reticulum protein, calreticulin, is transported into the acrosome of rat sperm. *Exp. Cell Res.* **205**, 101–110 (1993). <https://doi.org/10.1006/excr.1993.1063>
46. S. de Mateo, J. Castillo, J.M. Estanyol, J.L. Balleca, R. Oliva, Proteomic characterization of the human sperm nucleus. *Proteomics* **11**, 2714–2726 (2011). <https://doi.org/10.1002/pmic.201000799>
47. G.R. Klinefelter, J.E. Welch, S.D. Perreault, H.D. Moore, R.M. Zucker, J.D. Suarez, N.L. Roberts, K. Bobseine, S. Jeffay, Localization of the sperm protein SP22 and inhibition of fertility in vivo and in vitro. *J. Androl.* **23**, 48–63 (2002)
48. S. Girotto, L. Cendron, M. Bisaglia, I. Tessari, S. Mammi, G. Zanotti, L. Bubacco, DJ-1 is a copper chaperone acting on SOD1 activation. *J. Biol. Chem.* **289**, 10887–10899 (2014). <https://doi.org/10.1074/jbc.M113.535112>
49. Y. Wang, Y. Sun, X. Zhao, R. Yuan, H. Jiang, X. Pu, Down-regulation of DJ-1 fails to protect mitochondrial complex I subunit NDUF53 in the testes and contributes to the asthenozoospermia. *Mediators Inflamm.* **2018**, 6136075–6136075 (2018). <https://doi.org/10.1155/2018/6136075>

50. C. O'Flaherty, D. Matsushita-Fournier, Reactive oxygen species and protein modifications in spermatozoa. *Biol. Reprod.* **97**, 577–585 (2017). <https://doi.org/10.1093/biolre/iox104>
51. D. Lee, A.R. Moawad, T. Morielli, M.C. Fernandez, C. O'Flaherty, Peroxiredoxins prevent oxidative stress during human sperm capacitation. *Mol. Hum. Reprod.* **23**, 106–115 (2017). <https://doi.org/10.1093/molehr/gaw081>
52. G.K. Chacko, Characterization of high-density lipoprotein binding sites in rat liver and testis membranes. *Biochimica et Biophysica Acta (BBA) - Lipids and Lipid Metab.* **795**, 417–426 (1984). [https://doi.org/10.1016/0005-2760\(84\)90093-6](https://doi.org/10.1016/0005-2760(84)90093-6)
53. E. Akerlof, H. Jornvall, H. Slotte, A. Pousette, Identification of apolipoprotein A1 and immunoglobulin as components of a serum complex that mediates activation of human sperm motility. *Biochemistry* **30**, 8986–8990 (1991)
54. F. Odet, S. Gabel, R.E. London, E. Goldberg, E.M. Eddy, Glycolysis and mitochondrial respiration in mouse LDHC-null sperm. *Biol. Reprod.* **88**, 95 (2013). <https://doi.org/10.1095/biolreprod.113.108530>
55. F. Odet, C. Duan, W.D. Willis, E.H. Goulding, A. Kung, E.M. Eddy, E. Goldberg, Expression of the gene for mouse lactate dehydrogenase C (*Ldhc*) is required for male fertility. *Biol. Reprod.* **79**, 26–34 (2008). <https://doi.org/10.1095/biolreprod.108.068353>
56. T.W. Ijiri, M.L. Vadnais, A.M. Lin, A.P. Huang, W. Cao, T. Merdushev, G.L. Gerton, Male mice express spermatogenic cell-specific triosephosphate isomerase isozymes. *Mol. Reprod. Dev.* **80**, 862–870 (2013). <https://doi.org/10.1002/mrd.22217>
57. P.V. Danshina, C.B. Geyer, Q. Dai, E.H. Goulding, W.D. Willis, G.B. Kitto, J.R. McCarrey, E.M. Eddy, D.A. O'Brien, Phosphoglycerate kinase 2 (*PGK2*) is essential for sperm function and male fertility in mice. *Biol. Reprod.* **82**, 136–145 (2010). <https://doi.org/10.1095/biolreprod.109.079699>
58. M. Nakamura, S. Okinaga, K. Arai, Metabolism of pachytene primary spermatocytes from rat testes: pyruvate maintenance of adenosine triphosphate level. *Biol. Reprod.* **30**, 1187–1197 (1984)
59. B.T. Storey, F.J. Kayne, Energy metabolism of spermatozoa. V. The Embden-Myerhof pathway of glycolysis: activities of pathway enzymes in hypotonically treated rabbit epididymal spermatozoa. *Fertil. Steril.* **26**, 1257–1265 (1975)